

## Solution Cross-Linked Natural Rubber (NR)/Clay Aerogel Composites

Tassawuth Pojanavaraphan,<sup>†,§</sup> Lei Liu,<sup>†</sup> Deniz Ceylan,<sup>‡</sup> Oguz Okay,<sup>‡</sup>  
Rathanawan Magaraphan,<sup>§</sup> and David A. Schiraldi<sup>\*,†</sup>

<sup>†</sup>Department of Macromolecular Science and Engineering, Case Western Reserve University, Cleveland, Ohio 44106-7202, United States, <sup>‡</sup>Department of Chemistry, Istanbul Technical University, 34469 Maslak, Istanbul, Turkey, and <sup>§</sup>Polymer Processing and Polymer Nanomaterials Research Unit, The Petroleum and Petrochemical College, Chulalongkorn University, Bangkok 10330, Thailand

Received October 27, 2010; Revised Manuscript Received January 12, 2011

**ABSTRACT:** Aerogels are structural materials with ultralow bulk densities (often less than 0.1 g cm<sup>-3</sup>), which stand out as good candidates for a variety of applications. In the present study, natural rubber (NR)/clay aerogel composites were produced by freeze-drying of the aqueous aerogel precursor suspensions, followed by solution cross-linking of the aerogel samples in benzene using sulfur monochloride (S<sub>2</sub>Cl<sub>2</sub>) as a cross-linking agent. The influences of cross-linking conditions, i.e., cross-linker concentration and reaction temperature, as well as polymer loading on the aerogel structure and properties were investigated. 1% (v/v) of S<sub>2</sub>Cl<sub>2</sub> and reaction temperature of -18 °C were found to be the optimum conditions for producing a strong and tough rubber composite; the 2.5 wt % NR aerogel, for example, after being cross-linked, exhibited a compressive modulus of 1.8 MPa, 26 times higher than that of the neat control. These favorable mechanical properties are attributed to the high local concentration of rubber and S<sub>2</sub>Cl<sub>2</sub> in the freeze-dried structures, giving rise to the high cross-linking efficiency. Increasing the rubber concentration led to a substantial increase in the mechanical strength, in accord with the changes in microstructure and degree of cross-linking. The swelling capacity of the NR aerogels decreased with either increasing the cross-linker concentration or decreasing the weight fraction of rubber. Cross-linking of the rubber aerogels brought about increased thermal stability, consistent with restricted thermal motion of NR chains.

### Introduction

Layered silicates, especially sodium montmorillonite (Na<sup>+</sup>-MMT) and its organically modified analogues, have been extensively used as reinforcing fillers in polymer composites because of their unique characteristics of nanoscopic dimensions and high aspect ratios (100–150) and broad availability.<sup>1,2</sup> The bulk properties in composites are known to be functions of the volume fraction, dispersion state, and orientation of the platelet particles as well as the inherent properties of the different components that constitutes the composites.<sup>2,3</sup> Aerogels are representatives of an emerging class of structural materials with ultralow densities as well as high porosity (void fractions of ~95%), which hold promise for a wide variety of applications ranging from packaging/insulating to absorption materials.<sup>4–12</sup> Through a robust and environmentally benign freeze-drying process, layered silicates can be converted into the “house of cards”-like aerogels, produced in the grain boundaries of ice crystals, with bulk densities typically in the range between 0.02 and 0.15 g cm<sup>-3</sup>.<sup>4–13</sup> Clay aerogels typically possess lamellar architectures with layer thicknesses and distances between layers in the range of 1–5 and 20–100 μm, respectively.<sup>13</sup> As the pristine clay aerogels are fragile and lack an efficient energy dissipation mechanism in their frameworks, the addition of a polymeric component and/or reinforcing fibers is essential for optimizing their structural integrity and creating materials with mechanical properties similar to those of typical foamed polymers.<sup>4–13</sup>

In previous studies, natural rubber (NR)/clay aerogel composites were produced by freeze-drying aqueous suspensions that were prepared using a sulfur-based cure system (conventional

vulcanization).<sup>14,15</sup> Although the compressive moduli of conventionally vulcanized NR/clay aerogel composites increased as a function of clay volume fraction, those values were somewhat low (19–35 kPa) compared to other aerogels reported to date. These low moduli were attributed to the low thermal conductivity of the aerogel materials, which in turn led to an incomplete vulcanization of the rubber matrix when thermally cured.

Previous work has shown that sulfur monochloride (S<sub>2</sub>Cl<sub>2</sub>), a liquid at room temperature and soluble in organic solvents, can be an effective solution cross-linker for butyl rubber (PIB), even at very low polymer concentrations.<sup>16–20</sup> The organogels thus obtained displayed the distinct characteristics in terms of internal morphology, degree of toughness, and rate of response against the external stimuli (solvent change), which strongly depend on a large number of factors such as preparation temperature (*T*<sub>prep</sub>), freezing rate, choice of a cross-linking medium, and concentration of S<sub>2</sub>Cl<sub>2</sub>.<sup>16–20</sup> For instance, gel particles prepared in the frozen state using benzene as the cross-linking medium exhibited a macroporous structure, consisting of large interconnected pores, with rapid responsiveness and a high degree of toughness, allowing compression up to 100% strain without any crack development.<sup>17–20</sup> The present study aims to utilize S<sub>2</sub>Cl<sub>2</sub> as a solution cross-linking agent for aerogel materials based on NR and Na<sup>+</sup>-MMT clay, potentially generating highly stiff/tough NR-based foamlike materials without significant bulk densification. A series of cross-linked NR/clay aerogel composites were produced, and their swelling capacities, mechanical behaviors, microstructures, and thermal properties were evaluated.

### Experimental Section

**Materials.** Natural rubber latex (~60% dry solid content) was provided by the Goodyear Tire & Rubber Co. (Akron, OH).

\*To whom correspondence should be addressed: e-mail das44@case.edu; Tel (216) 368 4243; Fax (216) 368 4202.

The cross-linking agent sulfur monochloride ( $S_2Cl_2$ ; Aldrich) and benzene, toluene, and methanol (Merck) were used as received. Montmorillonite (PGW grade) with a cation exchange capacity of 145 mequiv/100 g (Nanocor Inc.) was used without further modification. Deionized (DI) water was prepared using a Barnstead RoPure low-pressure, reverse osmosis system.

**Aerogel Preparation.** A 10% w/v clay aqueous suspension was initially prepared by blending 2.75 g of  $Na^+$ -MMT with 27.5 mL of DI water on the high speed setting of a Waring model MC2 mini laboratory blender for  $\sim 1$  min. Appropriate amounts of NR latex and DI water were then added with gentle mechanical stirring to create the NR/clay hydrogels comprising 5 wt % clay gel and different concentrations of NR, ranging from 2.5 to 10 wt %. For instance, 2.4 g of NR latex and 29 mL of DI water were mixed with the 10 wt % clay gel to produce 2.5 wt % NR/5 wt % clay dispersions. Once thoroughly mixed, the combined solutions were transferred to the cylindrical polystyrene vials and immediately frozen in a solid carbon dioxide/ethanol bath ( $\sim -80$  °C), before being dried for 4 days in the chamber of a VirTis Advantage EL-85 lyophilizer with a shelf temperature of 25 °C and an ultimate chamber pressure of 10  $\mu$ bar. As noted, wt % herein refers to the weight percentage of each component in the parent aqueous dispersion/gel, and the clay weight fraction was kept constant at 5 wt % in order to produce samples sufficiently robust to allow for accurate mechanical testing.<sup>10</sup>

**Solution Cross-Linking Process.** Benzene solutions of  $S_2Cl_2$  were chosen for conducting the solution cross-linking of the NR/clay aerogel composites (NR aerogels). Two sets of experimental conditions were performed: (A) as for the 2.5 wt % NR aerogels,  $S_2Cl_2$  concentration was varied between 0.25 and 5% (v/v), and the reactions were conducted at a given temperature ( $T_{prep}$  of either  $-18$  or  $18$  °C); (B) as for the 5 and 10 wt % NR aerogels, the  $S_2Cl_2$  concentration and  $T_{prep}$  were kept constant at 1% (v/v) and  $-18$  °C, respectively.

In a typical experiment, the aerogel samples were immersed in an excess benzene solution of  $S_2Cl_2$  of different concentrations. Preliminary studies showed that the aerogels immediately absorbed benzene to attain their equilibrium states. Thus, after 1 min of the immersion time, the samples together with the external solution were transferred to either a thermostated room ( $T_{prep}$  of 18 °C) or a freezer ( $T_{prep}$  of  $-18$  °C), and the cross-linking reactions were allowed to proceed for 24 h. Thereafter, the samples were taken out of the solution and were extracted with an excess of toluene at room temperature to wash out the soluble polymer and the unreacted  $S_2Cl_2$ . Finally, they were placed in methanol overnight, during which methanol was refreshed several times, and dried under vacuum at 40 °C. As noted, all the neat and cross-linked samples were kept in an acrylic desiccator before testing in order to prevent any moisture absorption.

**Characterizations.** Densities of the NR aerogels before and after the solution cross-linking were calculated by measuring the mass and dimensions using a Mettler Toledo AB204-S analytical balance and digital caliper, respectively.

Compression testing was conducted on the cylindrical specimens ( $\sim 20$  mm in diameter and height) using an Instron model 5565 universal testing machine, fitted with a 1 kN load cell, at a constant crosshead speed of 1 mm  $min^{-1}$ . The compressive modulus and toughness at a given strain were determined from the slope of the linear portion and the integrated area of the stress-strain curve, respectively. Three identical samples of each composition were tested for reproducibility, and the values were averaged to obtain the reported results.

Samples for scanning electron microscopy (SEM) were prepared by sputter-coating the fractured monoliths with a thin layer of palladium ( $\sim 50$  Å). Imaging, elemental mapping, and the energy dispersive X-ray (EDX) analyses were performed using a Quanta 3D 200i FE-SEM at an acceleration voltage of 5 kV.

Thermal properties were examined using a TGA Q500 (TA Instruments) under a nitrogen flow (40 mL  $min^{-1}$ ). Approximately 5 mg of samples was placed in a platinum pan and heated from ambient temperature to 600 °C at a rate of 10 °C  $min^{-1}$ .

The swelling capacity of the NR aerogels before and after the solution cross-linking was determined by following the weight and diameter of the samples immersed in toluene for at least 24 h. The equilibrium weight and volume swelling ratios, denoted as  $q_w$  and  $q_v$ , respectively, were calculated using the following equations:

$$q_w = \frac{m_{tol}}{m_{dry}} \quad (1)$$

$$q_v = \left( \frac{D_{tol}}{D_{dry}} \right)^3 \quad (2)$$

where  $m_{tol}$  and  $m_{dry}$  are the weights of the equilibrium swollen and dry NR aerogels, respectively, and  $D_{tol}$  and  $D_{dry}$  are the corresponding diameters. As noted, in order to dry the equilibrium swollen NR aerogels, they were first transferred into methanol overnight and then dried under vacuum.

The pore volume ( $V_p$ ) of the networks was estimated through uptake of methanol of the NR aerogels. Since methanol is a nonsolvent for NR, it only enters into the pores of the aerogel networks. Thus,  $V_p$  (mL of pores in 1 g of dry aerogel network) was calculated as

$$V_p = \frac{m_M - m_{dry}}{d_M m_{dry}} \quad (3)$$

where  $m_M$  is the weight of the NR aerogels immersed in methanol after 24 h and  $d_M$  is the density of methanol (0.792 g  $mL^{-1}$ ).

The cross-link density ( $V_e$ ) of the NR aerogels was determined in situ from the equilibrium swelling measurements at room temperature, on the basis of Flory–Rehner theory,<sup>2,14,15</sup> which assumes a phantom model to describe the elastic behavior of the swollen network:

$$V_e = - \frac{\ln(1 - \phi_r) + \phi_r + \chi \phi_r^2}{V_1 \left( \phi_r^{1/3} - \frac{\phi_r}{2} \right)} \quad (4)$$

$$\phi_r = \frac{\frac{w_d - f_{ins} w_i}{\rho_r}}{\frac{w_d - f_{ins} w_i}{\rho_r} + \frac{w_{sol}}{\rho_s}} \quad (5)$$

where  $V_e$  is the network chain density (mol  $cm^{-3}$ ),  $\chi$  is the Flory–Huggins interaction parameter (0.391),  $V_1$  is the molar volume of toluene (106.2  $cm^3 mol^{-1}$ ),  $\phi_r$  is the rubber volume fraction,  $w_d$  and  $w_i$  are the deswollen and initial weights of the NR aerogels, respectively,  $f_{ins}$  is the weight fraction of an insoluble component (only clay aerogel),  $\rho_r$  and  $\rho_s$  are the densities of rubber (0.92 g  $cm^{-3}$ ) and toluene (0.87 g  $cm^{-3}$ ), respectively, and  $w_{sol}$  is the weight of toluene taken up after 72 h. The values reported are averages of at least three test pieces per each composition ( $\sim 20$  mm diameter and  $\sim 10$  mm thick).

## Results and Discussion

The cross-linking efficiency of  $S_2Cl_2$  as a function of concentration and reaction temperatures ( $T_{prep}$ ) is discussed below. The evaluation was carried out using the 2.5 wt % NR aerogel as a reference. The results of experiments conducted on different weight fractions of NR, maintaining constant cross-linking

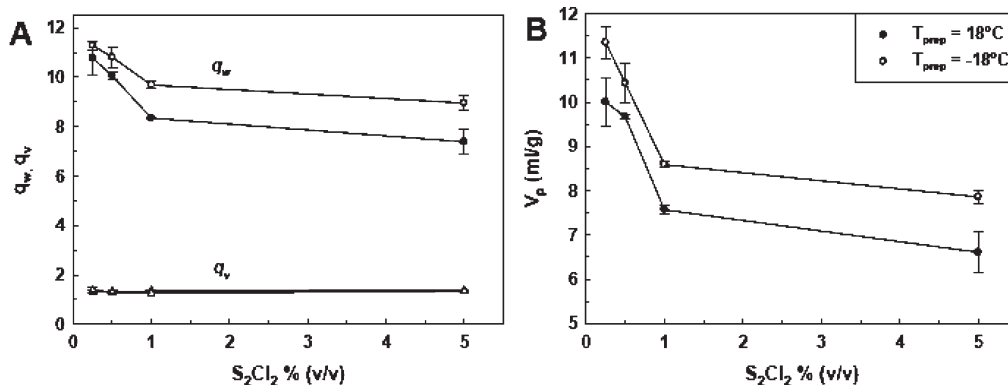


**Figure 1.** (A) Equilibrium weight  $q_w$  (circles) and volume  $q_v$  (triangles) swelling ratios of the 2.5 wt % NR aerogels in toluene shown as a function of  $S_2Cl_2$  concentration.  $T_{\text{prep}} = 18^\circ C$  (filled symbols) and  $-18^\circ C$  (open symbols). (B) Total volume of pores ( $V_p$ ) in 2.5 wt % NR aerogels estimated from the uptake of methanol shown as a function of  $S_2Cl_2$  concentration,  $T_{\text{prep}} = 18^\circ C$  (filled symbols) and  $-18^\circ C$  (open symbols).

conditions were also evaluated. A series of NR/clay aerogel materials were successfully produced by freeze-drying aqueous suspensions of these starting materials.

**1. Cross-Linking Efficiency of  $S_2Cl_2$ .** Since the NR aerogels were immersed into a large excess of  $S_2Cl_2$  solutions, it is reasonable to assume that some part of the solution (and thus of the  $S_2Cl_2$ ) remained outside of the aerogel phase. The amount of the  $S_2Cl_2$  in contact with the aerogel samples can be estimated as follows. By defining  $q_b$  to be the amount of benzene absorbed by 1 g of the NR aerogel, one can calculate the number of moles ( $n$ ) of  $S_2Cl_2$  in contact with 1 g of the NR aerogel using the following equations:

$$n_{S_2Cl_2} = \left(\frac{q_b}{d_b}\right) \left(\frac{S_2Cl_2\% \text{ v/v}}{100}\right) \left(\frac{d_{S_2Cl_2}}{MM_{S_2Cl_2}}\right) \quad (6)$$

$$q_b = \frac{m_b - m_{\text{dry}}}{m_{\text{dry}}} \quad (7)$$

where  $d_b$  and  $d_{S_2Cl_2}$  are the densities of benzene ( $0.877 \text{ g cm}^{-3}$ ) and  $S_2Cl_2$  ( $1.68 \text{ g cm}^{-3}$ ), respectively,  $MM_{S_2Cl_2}$  is the molar mass of  $S_2Cl_2$  ( $135 \text{ g mol}^{-1}$ ), and  $m_b$  is the weight of the swollen NR aerogel in benzene. The estimated amounts of  $S_2Cl_2$  in contact with 1 g of the 2.5 wt % NR aerogel were calculated as a function of  $S_2Cl_2$  concentrations in benzene; these are given in Table 1 of the Supporting Information. The general trend observed is that increasing the  $S_2Cl_2$  content in benzene solution leads to a continuous increase in the mole and weight percentage of  $S_2Cl_2$  in contact with the NR aerogel, and thus a high degree of cross-linking is expected.

The swelling capacities of the 2.5 wt % NR aerogels in toluene are displayed in Figure 1A, where the equilibrium weight  $q_w$  (circles) and volume  $q_v$  (triangles) swelling ratios are plotted against the  $S_2Cl_2$  concentration. The filled and open symbols are the data points obtained from the 2.5 wt % NR aerogels cross-linked at  $T_{\text{prep}}$  of 18 and  $-18^\circ C$ , respectively. Independent of the temperature ( $T_{\text{prep}}$ ), the weight swelling ratio ( $q_w$ ) of the 2.5 wt % NR aerogels decreased slightly with increasing  $S_2Cl_2$  concentration, in accord with previous work.<sup>19</sup> The 2.5 wt % NR aerogels cross-linked at  $T_{\text{prep}} = -18^\circ C$  exhibit larger  $q_w$  than those prepared at  $18^\circ C$ , and this is illustrated by the existence of much larger pore volumes, templated by the macroscopic benzene crystals, after conducting the reaction at very low temperature.<sup>17–20</sup> In contrast, the volume swelling ratio ( $q_v$ ) remains unchanged after adjusting the above experimental parameters, and its value is much less than the weight

swelling ratio ( $q_w$ ). The relative values of  $q_w$  and  $q_v$  provide information regarding the internal structure of the networks in the swollen state.<sup>17,18</sup> This is due to the fact that the  $q_w$  includes the solvent locating in both pores and polymer region of the NR aerogel, while the  $q_v$  represents only the solvent in the polymer phase. Thus, the large difference between these two values reflects the great amount of solvent locating in the pores. Figure 1B shows the total volume of pores ( $V_p$ ), estimated from the uptake of methanol by the 2.5 wt % NR aerogels, plotted against the  $S_2Cl_2$  concentration and temperature  $T_{\text{prep}}$ . The total pore volume ( $V_p$ ) decreases with increasing the  $S_2Cl_2$  concentration, regardless of the  $T_{\text{prep}}$ . Further, the samples prepared at  $T_{\text{prep}}$  of  $-18^\circ C$  exhibit the  $V_p$  in the range of 8–11  $\text{mL g}^{-1}$ , being slightly higher than those formed at  $18^\circ C$ , which is around 7–10  $\text{mL g}^{-1}$ . In accord with Figure 1A, this is a consequence of the frozen zones inside the aerogel samples at  $-18^\circ C$ , acting as templates during the reactions.<sup>19</sup> These results are in good agreements with the swelling characteristics of the typical macroporous PIB gels, prepared under similar experimental conditions.<sup>17–20</sup>

The mechanical properties of the 2.5 wt % NR aerogels were probed by the compression tests, and the results were interpreted in terms of the compressive modulus and toughness at a given strain. Figure 2A shows the typical stress–strain curves of the 2.5 wt % NR aerogels formed at  $T_{\text{prep}} = -18^\circ C$  under various  $S_2Cl_2$  concentrations. The line shapes follow the classical foam behavior in which a linear elastic region is followed by a horizontal plateau, and finally a densification region, which is similar to the curve of previously reported aerogels.<sup>7–13</sup> As noted, after being compressed up to 90%, the majority of the samples did not recover to their original size, even when the NR concentration was increased up to 10 wt %. The neat 2.5 wt % NR aerogel showed a compressive modulus and toughness at 30% strain of 70 and 2 kPa, respectively. After being cross-linked at  $-18^\circ C$ , the mechanical behavior was greatly improved; for instance, the samples formed at 1% (v/v)  $S_2Cl_2$  exhibited a compressive modulus and toughness at 30% strain of 1800 and 13 kPa, 26 and 7 times higher than those of the neat control, respectively (Figure 2B). The density of the aerogel increased only from 0.06 to 0.11  $\text{g cm}^{-3}$  (see Figure 2C) with cross-linking, so the specific modulus and specific toughness of these materials benefit greatly from the cross-linking process. Increasing the  $S_2Cl_2$  concentration beyond 1% (v/v) did not improve the mechanical properties of the cross-linked aerogels substantially but did increase the material density instead ( $\sim 0.12 \text{ g cm}^{-3}$ ). This behavior is probably due to cyclization reactions occurring

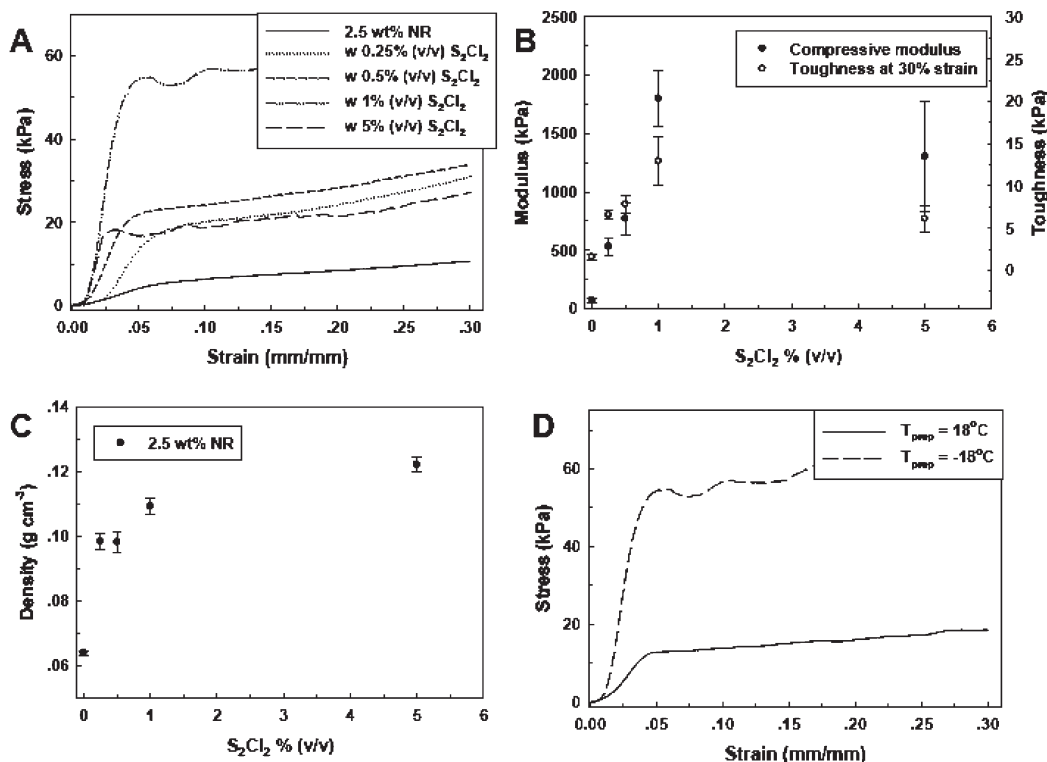


**Figure 2.** (A) Typical stress–strain curves of the 2.5 wt % NR aerogels cross-linked at various S<sub>2</sub>Cl<sub>2</sub> concentrations.  $T_{\text{prep}} = -18$  °C. (B) Changes in the compressive modulus (filled symbols) and toughness at 30% strain (open symbols) of the 2.5 wt % NR aerogels prepared at various S<sub>2</sub>Cl<sub>2</sub> concentrations.  $T_{\text{prep}} = -18$  °C. (C) Density of the 2.5 wt % NR aerogels shown as a function of the S<sub>2</sub>Cl<sub>2</sub> concentration,  $T_{\text{prep}} = -18$  °C. (D) Comparison of the stress–strain curves of the 2.5 wt % NR aerogels formed at different temperatures. S<sub>2</sub>Cl<sub>2</sub> = 1% (v/v).

between sulfur chloride and internal vinyl groups attached on the same polymer chains, which in turn limits the number of effective cross-links.<sup>16,19</sup>

Figure 2D compares the typical stress–strain curves of the 2.5 wt % NR aerogels cross-linked at different temperatures. The S<sub>2</sub>Cl<sub>2</sub> content was kept constant at 1% (v/v). The compressive modulus and toughness at 30% strain of the aerogel prepared at 18 °C were measured as 320 and 5 kPa, respectively. Increasing the reaction temperature from -18 to 18 °C led to a 6- and 3-fold decrease in the compressive modulus and toughness at 30% strain of the NR aerogels, respectively. This behavior demonstrates the much higher cross-linking efficiency of S<sub>2</sub>Cl<sub>2</sub> at very low reaction temperature as compared to that at ambient conditions. It is reasonable to expect that as the reaction solution is cooled below the freezing point of benzene (5.5 °C), both the rubber chains and S<sub>2</sub>Cl<sub>2</sub> molecules are excluded from the benzene crystals and accumulate to form the unfrozen regions. The reduced rate of reaction at low temperature would be compensated by the increased concentration of rubber and S<sub>2</sub>Cl<sub>2</sub> in the reaction zones, leading to the formation of dense rubber domains surrounding the benzene crystals.<sup>17–20</sup> If the cross-linking is conducted at ambient temperature, no freezing concentration of the reaction solution occurs, causing the rubber concentration in the reaction zones to be less than that of the apparently frozen reaction system,<sup>18</sup> limiting the formation of effective cross-links between the rubber chains. The hydrolysis of S<sub>2</sub>Cl<sub>2</sub> molecules is also more probably at ambient temperature as well.<sup>19</sup> It can be inferred from this result that, by conducting the reaction at 1% (v/v) of S<sub>2</sub>Cl<sub>2</sub> and  $T_{\text{prep}} = -18$  °C, the swelling capacities and mechanical integrity of the 2.5 wt % NR aerogels are optimally developed.

The degree of cross-linking ( $V_c$ ) of the 2.5 wt % NR aerogels, shown in Figure 3, varies linearly with the concentration

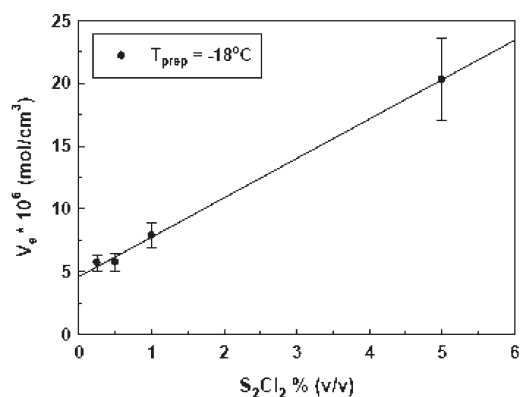


**Figure 3.** Variation of the degree of cross-link ( $V_c$ ) of the 2.5 wt % NR aerogels as a function of S<sub>2</sub>Cl<sub>2</sub> concentration.  $T_{\text{prep}} = -18$  °C. The line is only a guide to the eye.

of S<sub>2</sub>Cl<sub>2</sub>. This is expected since the calculated cross-link density should be related to the modulus of elasticity of the samples.<sup>2</sup> Although the highest cross-link density is attained at 5% (v/v) of S<sub>2</sub>Cl<sub>2</sub>, most of the sulfur bridges are originated from the cyclization reactions occurring between sulfur chloride and internal vinyl groups attached on the same rubber chains; those linkages are not expected to be a major source of the reinforcement for the 2.5 wt % NR aerogels.

Figure 4 depicts the SEM images of the 2.5 wt % NR aerogels prepared at different levels of S<sub>2</sub>Cl<sub>2</sub>, with a  $T_{\text{prep}}$  of -18 °C. Taking the neat control as a reference, the image (Figure 4A) reveals a well-defined layered architecture that follows the direction of the growing ice crystals.<sup>4–13</sup> After being cross-linked with 0.25 and 0.5% (v/v) of S<sub>2</sub>Cl<sub>2</sub>, it is seen that the lamellar structure collapses slightly, and the regularity of space between each layer is reduced. This structural

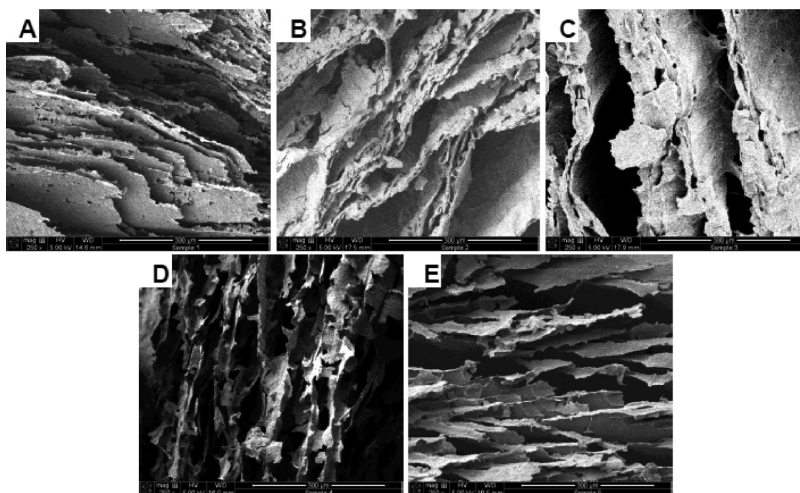


**Figure 4.** SEM images of the 2.5 wt % MR aerogels cross-linked at different levels of  $S_2Cl_2$ : (A) the neat control; (B) 0.25% (v/v); (C) 0.5%; (D) 1% (v/v); (E) 5% (v/v).  $T_{prep} = -18\text{ }^\circ\text{C}$ .

behavior demonstrates the relaxation of the constituent materials, making up the layers, after swelling of the aerogel samples in the organic solvent (benzene) prior to the solution cross-linking.<sup>11</sup> As there is an insufficient amount of  $S_2Cl_2$  for producing the stable polymer phase within a practical time, many of the structures collapse as a result of the structural relaxation upon absorption of benzene. When the  $S_2Cl_2$  concentration is increased to 1 and 5% (v/v), the lamellar morphology remains unchanged over the entire cross section of the samples, and the sheets are somewhat rougher; increased cross-linking efficiency in the polymer-rich unfrozen channels at much higher  $S_2Cl_2$  concentration appears to give rise to the formation of denser polymer domains, sufficiently strong to compromise the structural relaxation. A lack of the structural integrity is also evidenced for the NR aerogels prepared at  $T_{prep} = 18\text{ }^\circ\text{C}$  (not shown), even though the  $S_2Cl_2$  content was kept constant at 1% (v/v). This again reflects the low cross-linking efficiency at high reaction temperature, as mentioned earlier. EDX spectroscopy was conducted to monitor the success of the solution cross-linking of 2.5 wt % NR aerogels at  $T_{prep}$  of  $-18\text{ }^\circ\text{C}$ , and the results are collected in Table 2 of the Supporting Information. As expected, increasing the  $S_2Cl_2$  concentration leads to a linear increase in the weight ratios of the S/C and S/Si, which is from 0.1 to 0.8 and 0.2 to 2.3, respectively.

**2. Effect of the NR Concentration.** The incorporation of polymeric binders into the pristine clay aerogels is an effective approach for producing the rigid, foamlake materials.<sup>7–13</sup> Increasing the NR concentration we believe should lead to the formation of the interpenetrating cocontinuous networks, in which the layers appear to be connected by a web of polymer, giving us the significant improvement in the material properties.

The solution cross-linking of NR aerogels, comprising 5 and 10 wt % of NR, was conducted at 1% (v/v) of  $S_2Cl_2$  and  $T_{prep}$  of  $-18\text{ }^\circ\text{C}$ . The estimated amount of  $S_2Cl_2$  in contact with 1 g of the 5 and 10 wt % NR aerogels was calculated using eqs 6 and 7 and is collected in Table 3 of the Supporting Information. It is seen that increasing the weight fraction of NR slightly increases the amount of benzene uptake ( $q_b$ ) and, thereby, the weight percentage of  $S_2Cl_2$  in contact with 1 g of the samples. Figure 5 illustrates a linear dependency of the bulk densities of the neat and cross-linked NR aerogels on the weight fraction of NR. The bulk density of NR aerogels increases from 0.06 to 0.13  $\text{g cm}^{-3}$ , as the weight fraction of NR is increased up to 10 wt %. At the same time,

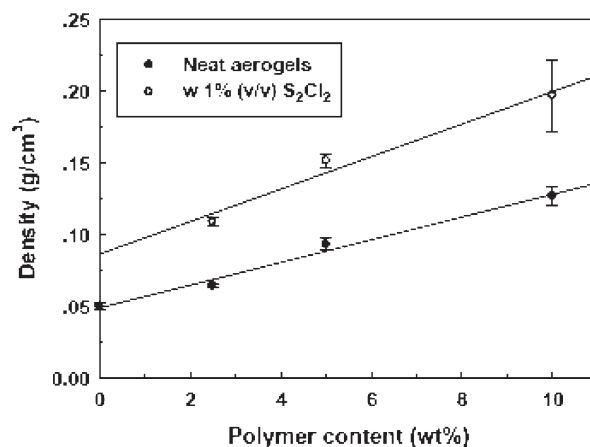


**Figure 5.** Bulk densities of NT aerogels before (filled symbols) and after the cross-linking reaction (open symbols) shown as a function of NR concentration.  $T_{prep} = -18\text{ }^\circ\text{C}$ .  $S_2Cl_2 = 1\%$  (v/v).

the cross-linked samples have the bulk density in the range of 0.11–0.20  $\text{g cm}^{-3}$ , being relatively higher than that of the neat controls, as expected.

The influence of rubber concentration on the materials mechanical properties is shown in Figure 6, where the stress–strain behaviors (A), compressive modulus (B), and toughness at 30% strain (C) of the neat and cross-linked NR aerogels are given. The general trend is that the samples containing relatively higher weight fraction of solid matter are stiffer than those lacking sufficient solid content to build the robust structures.<sup>10</sup> For instance, the compressive modulus is increased from 70 to 300 kPa, as the amount of NR increases from 2.5 to 10 wt %. However, this increase is not significant and limited by the lack of structural integrity of the rubber domain. It is therefore of considerable importance to create a large number of effective cross-links between the rubber chains in order to improve the rigidity of the NR aerogels and to promote the appreciable load transfer under stress. Results for compression tests of the cross-linked samples are shown in Figure 6B,C. It is seen that the compressive modulus and toughness at 30% strain of the cross-linked NR aerogels are increased by a factor of 15–27 $\times$  and 6–8 $\times$ , respectively, depending on the weight fraction of NR, as compared to those of the neat controls. Not surprisingly, the highest rigidity is observed for the

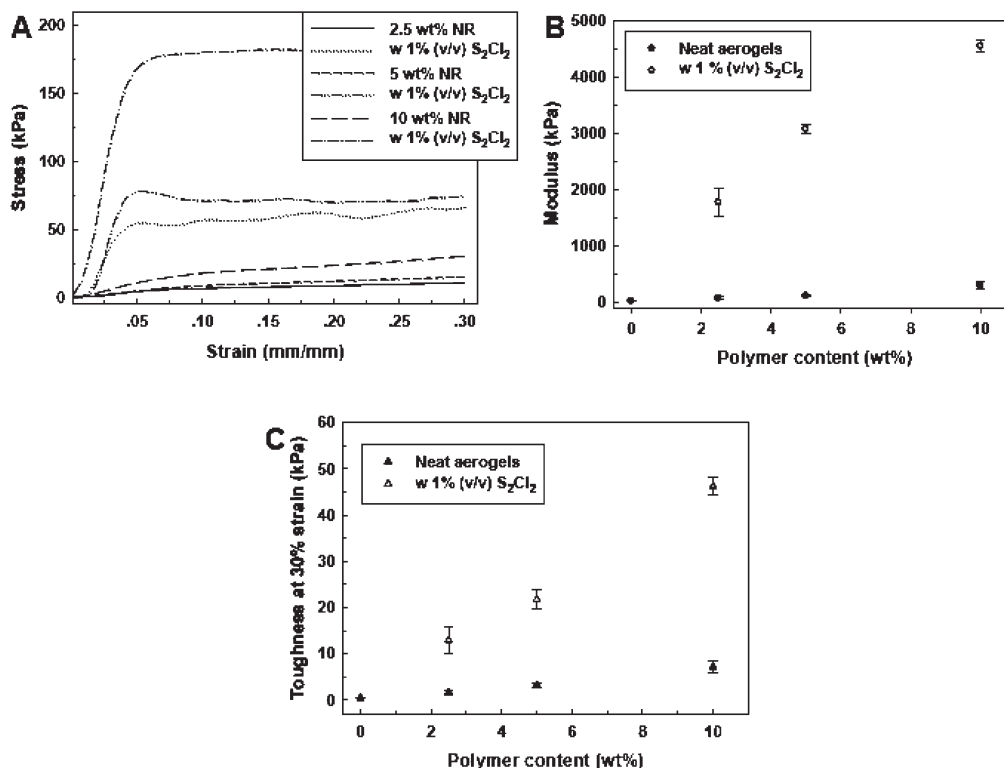


**Figure 6.** (A) Typical stress–strain curves of the neat and cross-linked NR aerogels, containing different weight fractions of NR, as indicated. (B, C) Compressive modulus (circles) and toughness at 30% strain (triangles) of the neat and cross-linked NR aerogels plotted as a function of NR concentration.  $T_{\text{prep}} = -18\text{ }^{\circ}\text{C}$ .  $\text{S}_2\text{Cl}_2 = 1\%$  (v/v).

cross-linked 10 wt % NR aerogel, which exhibits the compressive modulus and toughness at 30% strain of 4500 and 46 kPa, respectively. At the same time, the cross-linked aerogel density rises to  $0.20\text{ g cm}^{-3}$ , yielding the specific compressive modulus (modulus per unit weight) of  $22.5\text{ MPa cm}^3\text{ g}^{-1}$ , as compared to the values 16.4 and  $20.7\text{ MPa cm}^3\text{ g}^{-1}$  obtained using the cross-linked 2.5 and 5 wt % NR aerogels, respectively. As noted, the pristine clay aerogel, fabricated from a 5 wt % aqueous dispersion, has the compressive modulus of 20 kPa at a density of  $0.05\text{ g cm}^{-3}$ , which converts into the specific compressive modulus of  $0.4\text{ MPa cm}^3\text{ g}^{-1}$ .

Figure 7A illustrates the equilibrium weight  $q_w$  (circles) and volume  $q_v$  (triangles) swelling ratios of the NR aerogels in toluene plotted as a function of NR concentration. The filled and open symbols are the data points obtained from the neat and cross-linked NR aerogels, respectively. The volume swelling ratio ( $q_v$ ) of the neat NR aerogels increases slightly from 2 to 3, as the amount of NR matrix is increased from 2.5 to 10 wt %. In contrast, the weight swelling ratio ( $q_w$ ) does not change much with the weight fraction of NR, and the difference is limited by the length of experimental error. This difference is explained on the basis of a compromise between a reduction of the available pore volumes for the solvent to be drawn into and the increased absorption of solvent by the polymer domain, upon increasing the NR concentration. As noted, the volume swelling ratio ( $q_v$ ) only includes the solvent in the polymer region. Another evidence for a decrease in the static free volumes upon increasing the mass fraction of NR is shown in Figure 7B, where the total volume of pores ( $V_p$ ) of the NR aerogels is plotted against the NR concentration. It is seen that the total pore volume ( $V_p$ ) decreases from  $11.7$  to  $6.8\text{ mL g}^{-1}$  with increasing the weight fraction of NR, as expected. The swelling behaviors of the cross-linked NR aerogels follow the same pattern as those of the neat controls; however, the values, regarding the  $q_w$ ,  $q_v$ , and  $V_p$  are somewhat

lower, reflecting the formation of a large number of effective cross-links between the polymer chains, which in turn cause a restriction on the materials swelling capacity, particularly at high polymer loading. Figure 7C further illustrates a linear dependency of the cross-link densities ( $V_c$ ) of the NR aerogels on the weight fraction of NR, which is in good agreement with the compression data presented in Figure 6.

The microstructures of the 5 and 10 wt % NR aerogels before and after the cross-linking reactions are given in Figure 8. Before the solution cross-linking, it is apparent that increasing the weight fraction of NR results in the evolution of the aerogel structure from the highly lamellar morphology (Figure 8A), in which the layers distinctly separate, to the more continuous structure (Figure 8B), in which the layers are connected by a web of polymer. The appearance of the complete, interpenetrating networks at high mass fraction of solid matter is the primary reason for the vastly improved mechanical properties of the NR aerogels, as they are capable of supporting the applied mechanical loads. A similar result was reported by Gawryla et al.<sup>9</sup> for the low-density polymer/clay aerogel composites based on casein protein. The morphological transition is also evident in case of the cross-linked NR aerogels (see Figure 8C,D); however, the layers are quite coarse and rough. This again verifies the success of the solution cross-linking, which leads to the exceptional reinforcement of the NR aerogels. The EDX spectroscopy results (not shown) illustrate a slight decrease and increase in the S/C (from 0.4 to 0.2) and S/Si (from 0.8 to 1.8) weight ratios, respectively, with increasing the weight fraction of NR. Elemental mapping was performed on the cross-linked 10 wt % NR aerogel to identify the location of the S and Cl atoms, NR matrix, and clay aerogel, and the images are depicted in Figure 9. It is seen that both the S and Cl atoms are uniformly distributed over the investigated area and satisfactorily attach to the rubber domain, in accord

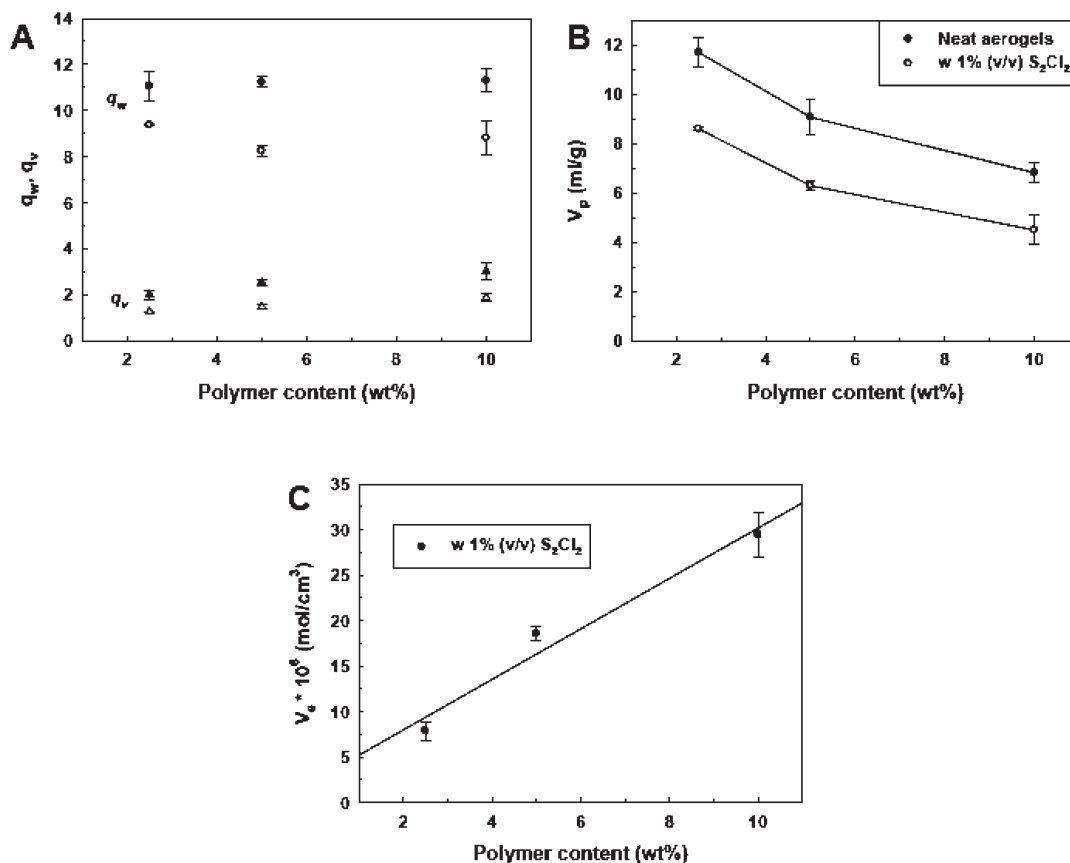


**Figure 7.** (A) Equilibrium weight  $q_w$  (circles) and volume  $q_v$  (triangles) swelling ratios of the neat (filled symbols) and cross-linked (open symbols) NR aerogels in toluene shown as a function of NR concentration.  $T_{\text{prep}} = -18^\circ\text{C}$ .  $\text{S}_2\text{Cl}_2 = 1\%$  (v/v). (B) Total volume of pores ( $V_p$ ) in the neat and cross-linked NR aerogels estimated from the uptake of methanol shown as a function of NR concentration,  $T_{\text{prep}} = -18^\circ\text{C}$ .  $\text{S}_2\text{Cl}_2 = 1\%$  (v/v). (C) Variation of the degree of cross-link ( $V_c$ ) of the NR aerogels as a function of NR concentration.  $T_{\text{prep}} = -18^\circ\text{C}$ .  $\text{S}_2\text{Cl}_2 = 1\%$  (v/v).

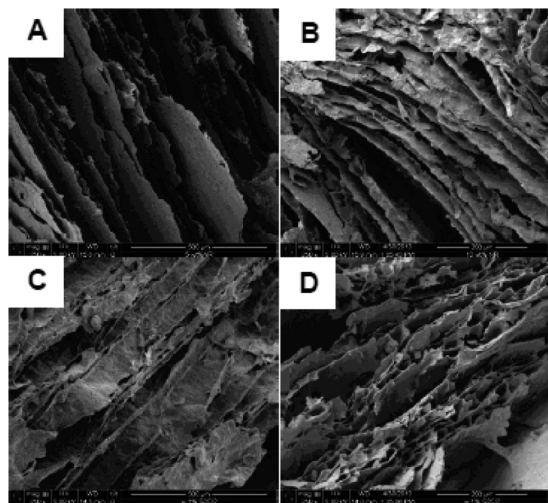


**Figure 8.** SEM micrographs of the 5 and 10 wt % NR aerogels: (A, B) before being cross-linked; (C, D) after being cross-linked.  $T_{\text{prep}} = -18^\circ\text{C}$  and  $\text{S}_2\text{Cl}_2 = 1\%$  (v/v).

with the reaction mechanism proposed by the Okay et al.<sup>16</sup> However, some of the S atoms are lying on the polymer-free surface of clay aerogel, as can be seen by the sulfur map, which is attributed to the high surface area of clay particles, which is capable of absorbing a part of curative on their surface.<sup>2,21</sup>

In Figure 10A,B, the TGA and DTG curves of the neat and cross-linked NR aerogels with various NR concentrations are

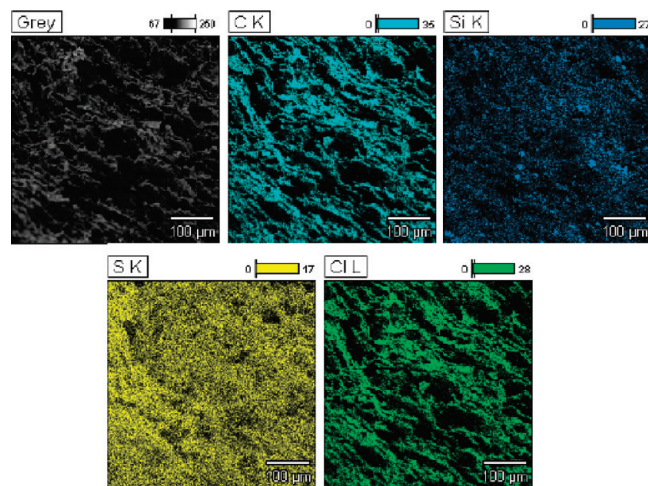


**Figure 9.** Elemental mapping of the 10 wt % NR aerogel cross-linked at 1% (v/v) of  $\text{S}_2\text{Cl}_2$  and  $T_{\text{prep}}$  of  $-18^\circ\text{C}$ .

given, respectively, and the overall results are collected in Table 1. The neat NR aerogels display a single step of weight loss in the range between 300 and 450  $^\circ\text{C}$ , which is related to the decomposition of NR phase. Increasing the NR concentration leads to a shift in the decomposition temperature ( $T_{d2}$ ) and rate of weight loss ( $dW/dT$ ) toward lower and higher values, respectively. This is not unexpected, as the actual percentage of clay aerogel (or char yield) decreases with increasing the weight fraction of NR. Therefore, the 10 wt % NR aerogel,

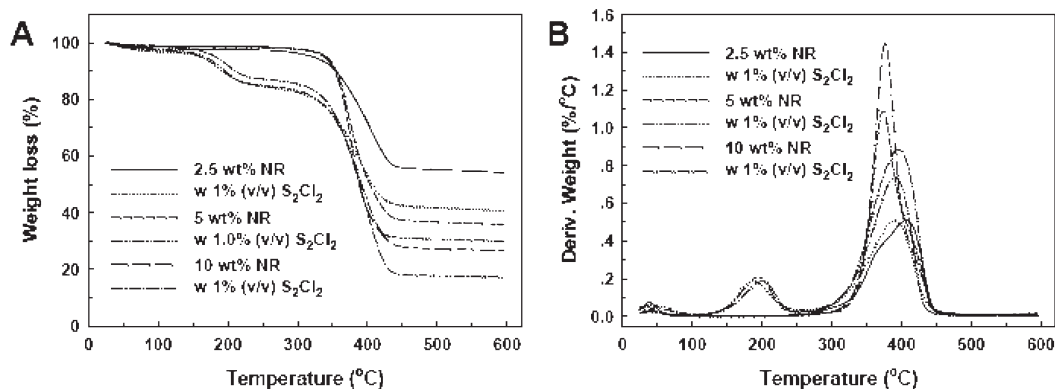


**Figure 10.** (A) TGA and (B) DTG thermograms of the neat and cross-linked NR aerogels, comprising various NR concentrations.  $T_{\text{prep}} = -18\text{ }^{\circ}\text{C}$  and  $\text{S}_2\text{Cl}_2 = 1\% \text{ (v/v)}$ .

**Table 1. Thermal Properties of the Studied Materials**

samples	$T_{d1}^a$ ( $^{\circ}\text{C}$ )	$W_1^b$ (%)	$T_{d2}^c$ ( $^{\circ}\text{C}$ )	$dW/dT^d$ (%/ $^{\circ}\text{C}$ )	$W_2^e$ (%)
2.5 wt % NR aerogel			407	0.5	43.3
w 1% (v/v) $\text{S}_2\text{Cl}_2$	191	12.0	391	0.5	43.9
5 wt % NR aerogel			374	1.1	62.4
w 1% (v/v) $\text{S}_2\text{Cl}_2$	194	12.6	391	0.7	54.3
10 wt % NR aerogel			377	1.4	71.7
w 1% (v/v) $\text{S}_2\text{Cl}_2$	200	11.0	396	0.9	69.2

<sup>a</sup>The temperature at which the hydrogen chloride gas (HCl) was removed. <sup>b</sup>Weight loss at the temperature range of 150–250  $^{\circ}\text{C}$ . <sup>c</sup>The decomposition temperature of NR. <sup>d</sup>The maximum rate of weight loss. <sup>e</sup>Weight loss at the temperature range of 250–600  $^{\circ}\text{C}$ .

comprising the lowest percentage of clay aerogel, displays an inferior thermal stability compared to that of the 2.5 wt % NR aerogel. After being cross-linked with  $\text{S}_2\text{Cl}_2$ , the thermal behavior of the NR aerogels shows a two-step weight loss process. The first step, observed in the range between 150 and 250  $^{\circ}\text{C}$ , is associated with the elimination of hydrogen chloride (HCl) gas,<sup>23</sup> which slightly lowers the onset decomposition of NR ( $T_0$ ); for instance, the  $T_0$  value is reduced from 355 to 350  $^{\circ}\text{C}$  when the 10 wt % NR aerogel was cross-linked. The appearance of HCl gas was verified by a decrease in the pH value of DI water from 8.4 to 5.7 upon the isothermal heating of the cross-linked sample in a three neck round-bottomed flask at 220  $^{\circ}\text{C}$  under a mild flow of  $\text{N}_2$  for 24 h. In the second step, it is apparent that the decomposition rate ( $dW/dT$ ) of the cross-linked samples is relatively lower than that of the neat controls, and the value of  $T_{d2}$  is now nearly the same, i.e., in the range between 391 and 396  $^{\circ}\text{C}$ , which is likely the decomposition range of the cross-linked NR, regardless of the weight fraction of clay aerogel. Therefore, it can be inferred that the cross-linked NR aerogels are more thermally stable than the neat controls, as the existence of sulfur bridges restricts the thermal motion of the rubber chains.

Independent of the solution cross-linking, there is small discrepancy existing between the theoretical (based on the starting material weights) and actual (calculated from the TGA mass loss, i.e.,  $W_1$  and  $W_2$ ) values of the organic matter in the dried composites (see Table 4 of the Supporting Information). This signifies that all of the organic matters were completely removed during the TGA analysis, leaving behind the char yield which is close to the actual percentage of inorganic clay aerogel, determined gravimetrically. Further, because of the highly porous internal structures, the polymer-free clay aerogel and low-density polymer/clay aerogel composites exhibit the thermal insulation properties similar to those of conventional insulating foams.<sup>9</sup> This low thermal conductivity is reflected in the value of  $T_{d2}$ , being

relatively higher than that of the typical NR matrix, which is around 374  $^{\circ}\text{C}$ .<sup>23</sup>

## Conclusions

A series of low density NR/clay aerogel composites were fabricated through a simple freeze-drying of the corresponding aqueous dispersions, followed by the solution cross-linking in benzene using  $\text{S}_2\text{Cl}_2$  as a cross-linking agent. Effects of the experimental conditions, viz.  $\text{S}_2\text{Cl}_2$  concentration and  $T_{\text{prep}}$ , on the structure and properties of the 2.5 wt % NR aerogel were initially investigated, and it was found that 1% (v/v) of  $\text{S}_2\text{Cl}_2$  and  $T_{\text{prep}}$  of  $-18\text{ }^{\circ}\text{C}$  were very effective for improving the mechanical properties, without affecting the microstructure. This behavior was explained by the high cross-linking efficiency of  $\text{S}_2\text{Cl}_2$  even at very low reaction temperatures. Increasing the  $\text{S}_2\text{Cl}_2$  content beyond this point did not further improve the materials properties but rather increased the bulk density. The weight fraction of NR was recognized as another crucial factor that influences the properties of the NR aerogels, since the structural integrity and bulk density were ultimately related to the total solids content of these materials. Increasing the weight fraction of NR from 2.5 to 10 wt % led to the structural changes from the highly lamellar morphology to the more continuous networks that confer the materials with much higher compressive modulus, connectivity, and density. At the same time, the reinforcing effect is even more prominent when the samples were cross-linked with 1% (v/v) of  $\text{S}_2\text{Cl}_2$  at  $T_{\text{prep}} = -18\text{ }^{\circ}\text{C}$ . The swelling capacity of the NR aerogels decreased with either increasing the  $\text{S}_2\text{Cl}_2$  concentration or decreasing the weight fraction of NR. TGA studies revealed that the cross-linked NR aerogels were more thermally stable than the neat controls, although the HCl (gas) was evolved after the certain degree of decomposition. Besides, the organic matters decomposed completely during the analysis, leaving behind the char yield that is close to the actual percentage of the inorganic clay aerogel. It is suggested that the developed foamlike materials are very promising for a wide variety of applications, where the low density and advanced mechanical behavior are of great importance.

**Acknowledgment.** Financial support from the Royal Golden Jubilee Ph.D. Program is greatly appreciated (PHD/0088/2549).

**Supporting Information Available:** Tables 1–4. This material is available free of charge via the Internet at <http://pubs.acs.org>.

## References and Notes

- (1) Bordes, P.; Pollet, E.; Avérous, L. *Prog. Polym. Sci.* **2009**, *34*, 125–155.



- (2) Valentín, J. L.; Mora-Barrantes, I.; Carretero-González, J.; López-Manchado, M. A.; Sotta, P.; Long, D. R.; Saalwächter, K. *Macromolecules* **2010**, *43*, 334–346.
- (3) Manitiu, M.; Horsch, S.; Gulari, E.; Kannan, R. M. *Polymer* **2009**, *50*, 3786–3796.
- (4) Somlai, L. S.; Bandi, S. A.; Schiraldi, D. A. *AIChE J.* **2006**, *52*, 1–7.
- (5) Bandi, S.; Bell, M.; Schiraldi, D. A. *Macromolecules* **2005**, *38*, 9216–9220.
- (6) Bandi, S.; Schiraldi, D. A. *Macromolecules* **2006**, *39*, 6537–6545.
- (7) Arndt, E. M.; Gawryla, M. D.; Schiraldi, D. A. *J. Mater. Chem.* **2007**, *17*, 3525–3529.
- (8) Finlay, K.; Gawryla, M. D.; Schiraldi, D. A. *Ind. Eng. Chem. Res.* **2008**, *47*, 615–619.
- (9) Gawryla, M. D.; Nezamzadeh, M.; Schiraldi, D. A. *Green Chem.* **2008**, *10*, 1078–1081.
- (10) Gawryla, M. D.; van der Berg, O.; Weder, C.; Schiraldi, D. A. *J. Mater. Chem.* **2009**, *19*, 2118–2124.
- (11) Gawryla, M. D.; Schiraldi, D. A. *Macromol. Mater. Eng.* **2009**, *294*, 570–574.
- (12) Johnson, J. R., III; Spikowski, J.; Schiraldi, D. A. *ACS Appl. Mater. Interfaces* **2009**, *1*, 1305–1309.
- (13) Gawryla, M. D.; Liu, L.; Grunlan, J. C.; Schiraldi, D. A. *Macromol. Rapid Commun.* **2009**, *30*, 1669–1673.
- (14) Pojanavaraphan, T.; Magaraphan, R. *Eur. Polym. J.* **2008**, *44*, 1968–1977.
- (15) Pojanavaraphan, T.; Schiraldi, D. A.; Magaraphan, R. *Appl. Clay Sci.* **2010**, *50*, 271–279.
- (16) Okay, O.; Durmaz, S.; Erman, B. *Macromolecules* **2000**, *33*, 4822–4827.
- (17) Ceylan, D.; Okay, O. *Macromolecules* **2007**, *40*, 8742–8749.
- (18) Dogu, S.; Okay, O. *Polymer* **2008**, *49*, 4626–4634.
- (19) Tuncaboylu, D. C.; Okay, O. *Eur. Polym. J.* **2009**, *45*, 2033–2042.
- (20) Ceylan, D.; Dogu, S.; Karacik, B.; Yakan, S. D.; Okay, O. S.; Okay, O. *Environ. Sci. Technol.* **2009**, *43*, 3846–3852.
- (21) Kader, M. A.; Nah, C. *Polymer* **2004**, *45*, 2237–2247.
- (22) Lee, D.; Char, K. *Polym. Degrad. Stab.* **2002**, *75*, 555–560.
- (23) Pojanavaraphan, T.; Magaraphan, R. *Polymer* **2010**, *51*, 1111–1123.